

Performance of Kramers-Kronig Receivers in the Presence of Local Oscillator Relative Intensity Noise

Wenting Yi, *Student Member, IEEE*, Zhe Li, *Member, IEEE*, M. Sezer Erkılınç, *Member, IEEE*, Domanıç Lavery, *Member, IEEE*, Eric Sillekens, *Student Member, IEEE*, Daniel Semrau, *Student Member, IEEE*, Zhixin Liu, *Senior Member, IEEE*, Polina Bayvel, *Fellow, IEEE*, and Robert I. Killey, *Senior Member, IEEE*

Abstract— There is increasing interest in low-complexity coherent optical transceivers for use in short-reach fiber links. Amongst the simplest configurations is the heterodyne coherent receiver, using a 3-dB coupler to combine the signal with the local oscillator (LO) laser output, and a single photodiode for detection of each polarization.

In this paper, through numerical simulations, we investigate the impact of signal-signal beating interference (SSBI) and LO relative intensity noise (RIN) on the performance of such coherent transceivers. Specifically, we assess the performance of two methods to mitigate the SSBI: firstly, the use of high LO laser power and, secondly, the application of digital signal processing-based receiver linearization, specifically, the Kramers-Kronig (KK) scheme. The results indicate that, in the case of a RIN-free LO laser, a strong LO is effective in mitigating SSBI and achieves a similar performance to that of the KK algorithm. However, the required increase in LO-to-signal power ratio (LOSPR) is significant. For example, a 20 dB higher optimum LOSPR was observed in the 28 Gbaud dual polarization 16 QAM system at an optical signal-to-noise power ratio (OSNR) of 22 dB.

The drawback of using such a high LOSPR is the increased penalty due to RIN-LO beating terms, which we next investigated. The lower optimum LOSPR, and consequently the lower impact of LO RIN on the performance of the KK receiver lead to a reduction in the pre-FEC BER by over an order of magnitude for LO RIN levels above -140 dBc/Hz.

Index Terms— Coherent communications, heterodyne detection, Kramers-Kronig receiver, laser relative intensity noise, signal-signal beating interference

I. INTRODUCTION

THE continuous development of data-intensive applications such as cloud computing/storage services, high-definition video-on-demand and the Internet of Things requires a more efficient utilization of available optical bandwidth in the optical fiber communications infrastructure supporting these services

This work was supported by the UK EPSRC UNLOC EP/J017582/1 project and TRANSNET EP/R035342/1 project. (Corresponding author: Wenting Yi) Wenting Yi, Domanıç Lavery, Eric Sillekens, Daniel Semrau, Zhixin Liu, Polina Bayvel, and Robert I. Killey are with the Optical Networks Group, Department of Electronic and Electrical Engineering, University College London, London, WC1E 7JE, U.K. Zhe Li is with Finisar Corporation, USA. M. Sezer Erkılınç is with Fraunhofer HHI, Germany. (e-mail: w.yi.17@ucl.ac.uk; zhe.li@finisar.com; sezer.erkilinc@hhi.fraunhofer.de; d.lavery@ee.ucl.ac.uk; e.sillekens@ee.ucl.ac.uk; uceedfs@ucl.ac.uk; zhixin.liu@ucl.ac.uk; p.bayvel@ucl.ac.uk; r.killey@ucl.ac.uk).

[1]. In contrast to intensity modulation direct detection (IM/DD) transceivers, coherent technology enables the use of all degrees of freedom of the optical field for signaling, including the phase, amplitude and polarization [2], and thus, have been widely adopted for long-haul applications [3-5]. Due to its superiority in terms of performance, the use of coherent receivers is now being considered for short links, in particular for those requiring high throughput and spectral efficiency.

Conventional intradyne coherent receivers used for long-haul links require a polarization beam splitter/rotator, two 90° optical hybrids and four pairs of balanced detectors, followed by four analogue-to-digital converters (ADCs), which increase the complexity and cost in comparison to direct detection systems. To address the complexity issue, a heterodyne detection-based coherent receiver design has recently been proposed [6, 7], which employs, for each polarization, a single 3-dB coupler to combine signal and local oscillator (LO), and a single-ended photodiode followed by an ADC, as shown in Fig.1. This receiver architecture shows potential for cost-sensitive applications, e.g., short links which require high information spectral density.

In the heterodyne detection process, the signal-LO beating converts the optical signal to an electrical signal at an intermediate frequency (IF), which is, subsequently, digitally down-converted to baseband frequency. In the case of single-ended photodetection, as opposed to balanced detection, a performance limitation arises due to signal-signal beating interference (SSBI) induced by the nonlinear square-law detection of a photodiode. One possible solution is to leave a sufficient frequency guard band between the optical carrier and the signal [8]. However, with this approach, half of the bandwidth of the optical and electrical components is wasted [9]. An alternative approach is to use digital signal processing (DSP) based linearization techniques in the receiver. The Kramers-Kronig (KK) scheme, in particular, has been demonstrated to be effective in reconstructing the optical phase from the received signal's envelope provided that the local oscillator-to-signal power ratio (LOSPR) is sufficiently high to satisfy the minimum phase condition [6, 7, 9-16]. A third approach, investigated in [17], is to achieve linearization of the receiver without the requirement for additional DSP through the use of a sufficiently high LO power. In this case, the power of the unwanted signal-signal beating terms is negligible in

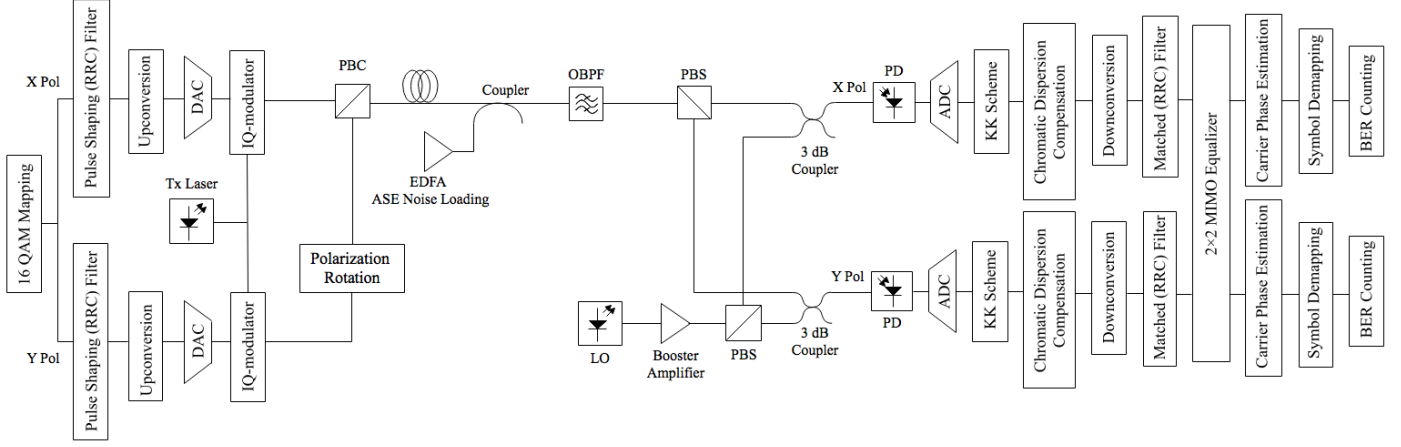


Fig. 1. Simulation setup for 28 Gbaud PDM 16-QAM heterodyne coherent detection system: RRC: root-raised-cosine; PBC: polarization beam combiner; EDFA: Erbium-doped fiber amplifier; OBPF: optical bandpass filter; PBS: polarization beam splitter; LO: local oscillator; PD: photodiode; MIMO: multiple-input multiple-output.

comparison to that of the desired signal-LO beating products.

In this paper, we analyze the operation of polarization division multiplexing (PDM) heterodyne coherent transceivers. The SSBI penalties, and their reduction by two techniques, namely, the use of a significantly higher LOSPR and the application of digital receiver linearization (using the Kramers-Kronig scheme), are assessed and compared. The level of the local oscillator laser's relative intensity noise (RIN) is shown to have a significant impact on the optimum choice of approach.

II. THEORY

A. Relative intensity noise

The RIN levels for lasers used in optical fiber communication links typically range from -160 to -130 dBc/Hz [18]. Low-cost lasers, such as distributed feedback (DFB) lasers, exhibit high relative intensity noise, typically above -140 dBc/Hz [19 - 21]. The relative intensity noise is the random intensity fluctuations in the instantaneous optical field stemming from the spontaneous emission noise, present even when the laser is biased well above the threshold. Relative intensity noise has a normal distribution, and its level is quantified as follows [22]:

$$RIN = \langle \delta P(t)^2 \rangle / \langle P(t) \rangle^2 \quad (1)$$

where $\langle \delta P(t)^2 \rangle$ refers to the variance of the power fluctuation, and $\langle P(t) \rangle^2$ represents the mean optical power squared. For a given RIN level, the variance of the power fluctuation increases proportionally to the mean LO power squared. Equation (1) gives the total relative intensity noise within the receiver bandwidth. Typically, the RIN level is normalized by the receiver bandwidth B , and is expressed in the units of dBc/Hz as follows:

$$RIN = 10 \log \left[\frac{\langle \delta P(t)^2 \rangle}{\langle P(t) \rangle^2} \cdot \frac{1}{B} \right] \quad (dBc/Hz) \quad (2)$$

In contrast to the amplified spontaneous emission (ASE) noise in amplified links, the RIN is frequency dependent, having a peak near the relaxation oscillation frequency of the

laser, typically around 1-10 GHz, and decreasing at higher frequencies [23]. As the injected current into the laser increases, the average relative intensity noise reduces, with the resonance peak reducing in magnitude and shifting to higher frequencies [22].

B. Beating interference

In optically amplified links, the performance of a heterodyne receiver, using a single-ended photodiode is limited by the combination of ASE noise from the inline amplifiers, the SSBI from the square-law photodetection and the LO RIN. The complex optical field in each polarization at the input of the corresponding photodiode can be written as:

$$E = E_{LO} + E_{Sig} + E_{RIN} + E_{ASE} \quad (3)$$

where the terms on the right-hand side are the optical fields of, respectively, the noise-free local oscillator, the signal, the local oscillator RIN and the ASE noise. Following square-law detection, the detected signal in each polarization is given by:

$$\begin{aligned} I &= R|E|^2 \\ &= R|E||E^*| \\ &= R(|E_{LO}|^2 + \underbrace{|E_{Sig}|^2}_{SSBI} + |E_{RIN}|^2 + |E_{ASE}|^2 \\ &\quad + \underbrace{2\text{Re}[E_{Sig}E_{LO}^*]}_{\text{signal-LO beating}} + 2\text{Re}[E_{Sig}E_{ASE}^*] + 2\text{Re}[E_{Sig}E_{RIN}^*] \\ &\quad + \underbrace{2\text{Re}[E_{RIN}E_{LO}^*]}_{\text{RIN-LO beating}} + \underbrace{2\text{Re}[E_{ASE}E_{LO}^*]}_{\text{ASE-LO beating}} + 2\text{Re}[E_{ASE}E_{RIN}^*]) \end{aligned} \quad (4)$$

where R is the responsivity of the photodiode, and $\text{Re}[x]$ signifies the real part of x . $|E_{LO}|^2$ is a direct current (DC) term which can be easily removed. The signal-LO beating product is the desired signal whereas all the other beating terms degrade the receiver sensitivity. As (4) suggests, the signal-LO beating term can be made significantly larger than the SSBI by increasing the LO laser output power. However, this results in an increased RIN-LO beating penalty [24, 25]. Therefore, there is a performance trade-off, when choosing the LO power,

between suppressing the SSBI, and avoiding significant RIN-LO beating interference. In the following sections, simulations assessing the impact of LO RIN and this trade-off in heterodyne receivers with single-ended photodetectors are described. We show how the use of digital linearization in the receiver can allow the use of lower LO power, hence reducing the level of the RIN-LO beating.

III. SIMULATION SETUP

The simulated setup is shown in Fig. 1. The simulations were carried out using MATLAB, with a single channel being considered. The system employed a 28 Gbaud PDM 16-QAM signal, at a gross data rate of 224 Gb/s, encoding a 2^{17} de Bruijn binary sequence. Lasers used in the transmitter and receiver were centered at 1550 nm with a linewidth of 1 MHz (unless otherwise stated), typical for the low-cost DFB lasers used in short-reach systems. At the transmitter, the signal was generated using root-raised-cosine (RRC) pulse shaping filters with 0.01 roll-off factor and a dual polarization IQ-modulator.

Random polarization rotation and differential group delay of the signal between transmitter and receiver were simulated. Since the use of inline optical amplification was assumed, ASE noise was added. The optical signal-to-noise power ratio (OSNR) is specified with a 0.1 nm (12.5 GHz) resolution bandwidth. At the receiver, the signal was first passed through a 28.42 GHz wide optical bandpass filter, eliminating out-of-band ASE noise. The PDM signal was demultiplexed by a polarization beam splitter (PBS), and, subsequently, combined with the aligned LO using polarization-maintaining 3-dB couplers. As mentioned in Section II. A, in practice, laser RIN varies with the laser's output power. Therefore, in order to allow the LO power to be varied while maintaining a constant RIN level, a noise-free booster amplifier was added after the LO laser to control the LO power. The local oscillator RIN was modelled with a frequency dependent property using (5) and the parameters listed in Table 1, taken from reference [22], multiplied by a frequency independent scaling parameter in order to allow the RIN value to be set to the desired value. The RIN is expressed in terms of its average spectral density over the receiver bandwidth (28.42 GHz). Fig. 2 shows the RIN spectrum at the average value of -139 dBc/Hz.

$$RIN = \frac{2R_{sp}[(\Gamma_N^2 + \omega^2) + G_N^2 P^2(1 + \gamma_e N/R_{sp}P) - 2\Gamma_N G_N P]}{P[(\Omega_R - \omega)^2 + \Gamma_R^2][(\Omega_R + \omega)^2 + \Gamma_R^2]} \quad (5)$$

TABLE I
LASER PARAMETERS

Parameter	Symbol	Value
Photon population	P	7.76×10^4
Carrier population	N	2.14×10^8
Spontaneous-emission rate	R_{sp}	$1.28 \times 10^{12} \text{ s}^{-1}$
Gain derivative ($\partial G/\partial N$)	G_N	$5.62 \times 10^3 \text{ s}^{-1}$
Small-signal carrier decay rate	Γ_N	$1.27 \times 10^9 \text{ s}^{-1}$

Relaxation-oscillation frequency	$\Omega_R/2\pi$	2.65 GHz
Relaxation-oscillation decay rate	Γ_R	$1.92 \times 10^9 \text{ s}^{-1}$
Carrier recombination rate	τ_e	$4.545 \times 10^9 \text{ s}^{-1}$

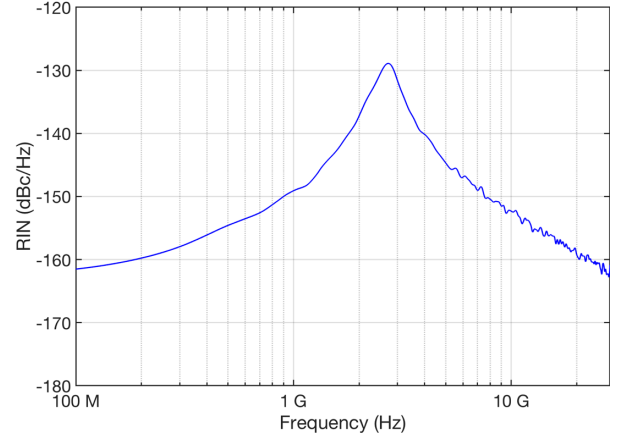


Fig. 2. The relative intensity noise spectrum at the average value of -139 dBc/Hz.

The frequency offset of the LO from the center of the signal spectrum was set to 14.28 GHz (0.51×28 GHz), and the combined signal and LO in each polarization were detected by a single-ended photodiode with a responsivity of 0.8 A/W. Shot noise and thermal noise due to the photodetection were included, though were found to have a negligible impact on system performance compared to the ASE noise and RIN. Unless otherwise specified, all electronic and optical components in the simulated system were ideal and noise-free. In the case of the Kramers-Kronig receiver, the KK algorithm was first applied to the signal, at a sampling rate of 6 Sa/symbol [26], following which dispersion compensation (applied in the case of 80 km transmission system as discussed in section IV.B), frequency down-conversion to baseband and RRC matched filtering were carried out. The two polarizations were then down-sampled to 2 Sa/symbol and passed through a 2×2 multiple-input multiple-output (MIMO) adaptive equalizer. The carrier phase estimation (CPE) was carried out using the QPSK-partitioning algorithm. Finally, symbol-to-bit demapping was performed using regular hard decision boundaries, and the bit-error-ratio (BER) and signal-to-noise ratio (SNR) were calculated. Aside from the absence of the KK algorithm, identical DSP was performed in the case of the receiver linearized using a high LO-to-signal power ratio.

IV. RESULTS AND DISCUSSION

In this section, we discuss and compare the performance of two methods (i.e., the application of the KK algorithm, and the use of high LO power) for suppressing the SSBI in the presence of LO relative intensity noise. The mitigation of SSBI impairment in back-to-back operation is first considered in section A, initially in the absence of, and, subsequently, in the

presence of LO RIN. In section A.3, an assessment of the impact of varying the laser linewidth, together with variation of the relative intensity noise, is presented. Following this, simulations of transmission over 80 km of standard single mode fiber were carried out, and the modelling results are analyzed in section B. In section C, the BER performance of the KK receiver in the presence of the ASE noise and RIN is compared with predictions based on the received signal SNR of an ideally linearized receiver. A concluding discussion of the results is presented in section D.

A. Performance in back-to-back setup

1) Without LO RIN

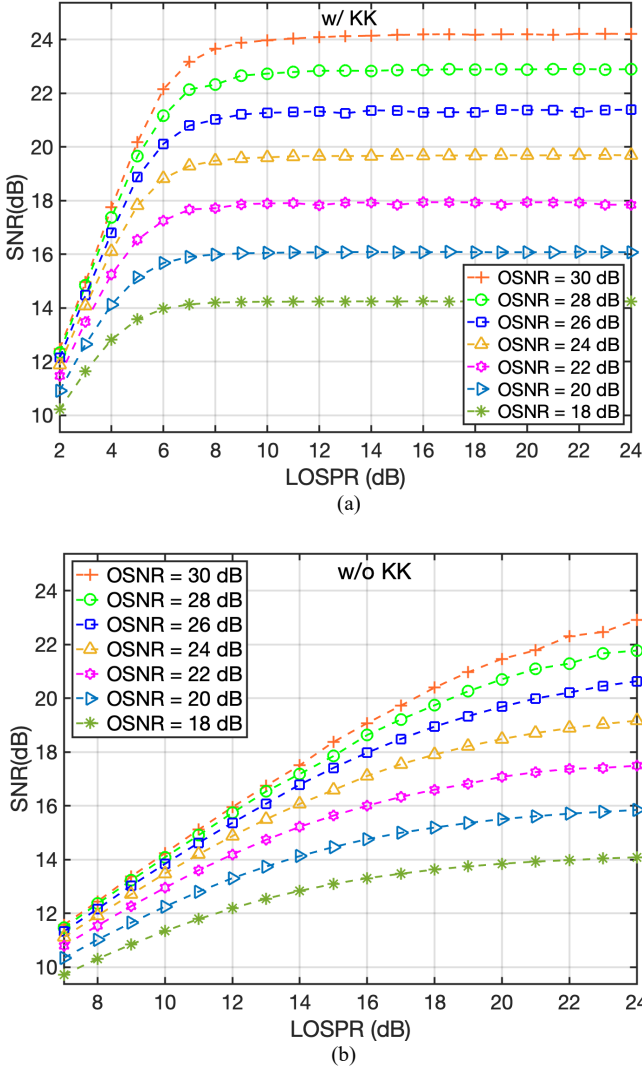


Fig. 3. SNR as a function of LOSPR at different OSNRs (a) with and (b) without the KK scheme.

In the scenario without LO laser RIN, the receiver sensitivity is degraded mainly by the ASE noise and SSBI. The SNR as a function of LO-to-signal power ratio at different OSNR values using the KK scheme is plotted in Fig. 3 (a). At LOSPRs below 10 dB, the SNR increases with the LOSPR, which indicates that the LO power is insufficiently high to ensure that the minimum phase condition is satisfied for the implementation of the KK

scheme. At LOSPRs of 10 dB and above, the system reaches the ASE-limited noise floor, leading to the constant SNR values. Therefore, the minimum phase condition is fulfilled at LOSPRs above 10 dB, and the SSBI is fully compensated.

Fig. 3 (b) presents the SNR with respect to LOSPR at different OSNRs for the receiver without the KK scheme. It can be observed that the increase in SNR with increasing LO power is much more gradual, although at high LOSPR values, effective SSBI suppression is achieved, as described in [17].

BER versus LOSPR, with and without the KK scheme, at an OSNR of 22 dB, is plotted in Fig. 4. Note that, in order to clearly show the BER floor in the plot, an OSNR of 22 dB was chosen; at higher OSNRs, the BER can go down to far lower values. The system reaches the BER floor of 2.6×10^{-4} at a LOSPR of ~ 10 dB when the KK algorithm is employed. Without the KK algorithm, the BER gradually decreases with increasing LOSPR, and converges to the same BER floor at a LOSPR of 30 dB, i.e., it requires ~ 20 dB higher LOSPR compared to the case with the KK scheme.

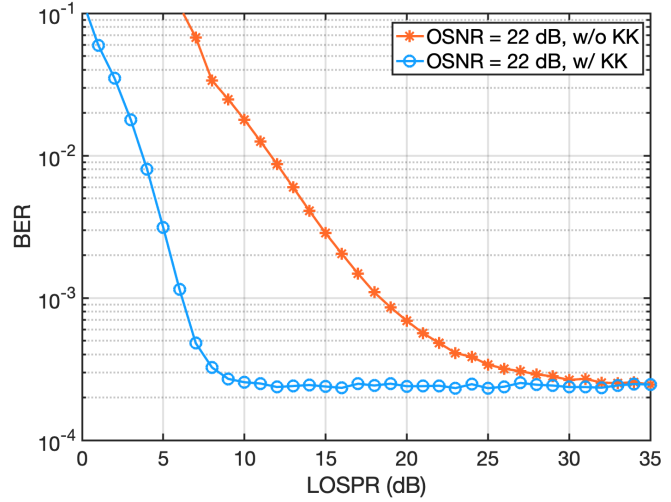


Fig. 4. BER versus LOSPR with and without the KK scheme at OSNR = 22 dB.

2) With LO RIN

In order to assess the impact of LO relative intensity noise on system performance, laser RIN was included in the simulations, with values (averaged across the receiver bandwidth) ranging from -170 dBc/Hz to -120 dBc/Hz.

BER versus LOSPR for the case with the KK algorithm at different RIN levels at an OSNR of 22 dB are plotted in Fig. 5 (open markers). At the lowest RIN level considered (-145 dBc/Hz), and with the KK scheme implemented, the BER reaches a minimum value of 2.9×10^{-4} at a LOSPR of 9 dB. The minimum BER is slightly higher than that without LO RIN. As the RIN increases from -145 dBc/Hz to -131 dBc/Hz, the optimum LOSPR (i.e., the value achieving minimum BER) shifts to lower values, and the minimum BER increases with increasing RIN. The reduction in the optimum LOSPR with increasing RIN arises as a result of the changing tradeoff between the minimum phase condition being unfulfilled and the noise due to the RIN-LO beating.

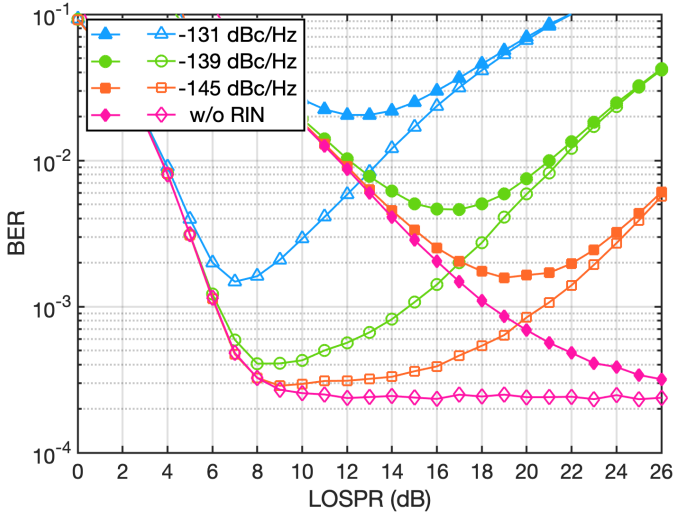


Fig. 5. BER versus LOSPR at different RIN levels at an OSNR of 22 dB. Solid markers refer to the case without the KK scheme whereas open markers refer to the case with the KK scheme.

The results can also be observed in Fig. 5 for the receiver without the KK scheme (solid markers). Due to the requirement for a high LO power to suppress the SSBI, the impact of laser RIN becomes much more significant. The reason is that the higher LO power needed for this receiver comes with the drawback of higher noise level in the electrical signal due to RIN-LO beating. Thus, the optimum LOSPR shifts to lower values with increasing RIN as a consequence of the shifting tradeoff between the unsuppressed SSBI and RIN-LO beating noise. Compared to the case with the KK scheme, the minimum BER is much higher at the same RIN level, for example 4.7×10^{-3} at -139 dBc/Hz (an order of magnitude higher than the minimum BER of 4×10^{-4} with the KK receiver at the same RIN level).

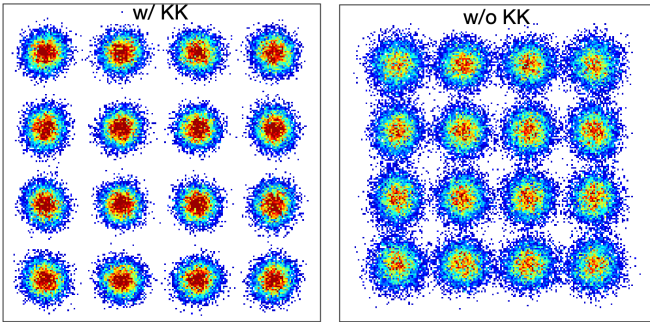


Fig. 6. Constellations at optimum LOSPR with (EVM = 13.4%) and without (EVM = 17.5%) the KK algorithm at an OSNR of 22 dB and a LO RIN of -139 dBc/Hz.

The received signal constellations with and without the KK scheme at optimum LOSPR, at a LO RIN level of -139 dBc/Hz and an OSNR of 22 dB, are presented in Fig. 6. At this RIN level, for the receiver without KK linearization, the optimum LOSPR is found to be 17 dB (Fig. 5), which results in higher amplitude RIN-LO beating products and unsuppressed SSBI interference, causing a more distorted constellation (an error vector magnitude (EVM) of 17.5%). In contrast, the use of the KK scheme reduces the optimum LOSPR to just 8 dB (Fig. 5),

leading to the lower RIN-LO beating, and consequently, a less distorted constellation (EVM = 13.4%).

The BER as a function of RIN at optimum LOSPR values, (i.e., optimized to achieve minimum BER values at each RIN level) at an OSNR of 22 dB is plotted in Fig. 7. In the absence of RIN (as shown in Fig. 4) or at a very low RIN level (e.g. -170 dBc/Hz shown in Fig. 7), a high LO power can suppress the SSBI in the receiver, achieving a similar system performance compared to the KK receiver, and thus, there is no need for digital linearization. However, the presence of LO RIN significantly degrades the system performance. Especially at RIN levels above -140 dBc/Hz, employing the KK receiver enables about an order of magnitude reduction in the BER. Simulations at OSNRs ranging from 18 to 30 dB were also carried out, with similar trends in the results being observed.

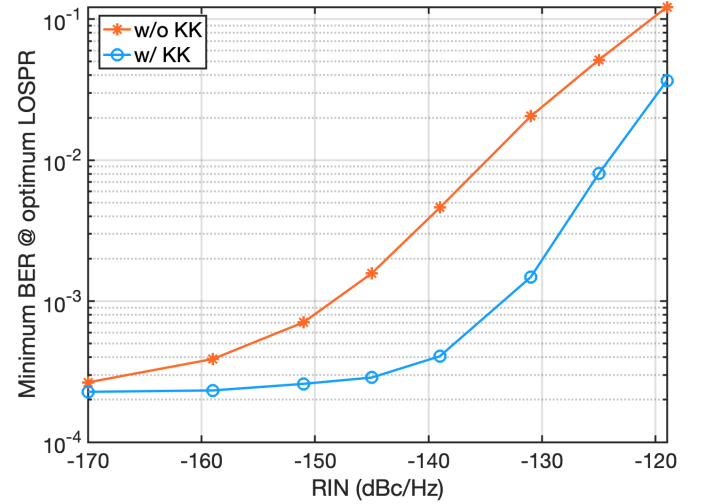


Fig. 7. Minimum BER versus RIN at optimum LOSPRs and OSNR of 22 dB in back-to-back operation.

3) Joint impact of laser linewidth and LO RIN

Low-cost lasers (e.g. DFB lasers) may suffer not only from high relative intensity noise, but also from high linewidth. In this section, the laser linewidth was varied, over the range 1 MHz to 5 MHz (the typical DFB linewidth range [19-21, 27, 28]), together with variation of the LO RIN, in back-to-back operation. The aim was to assess the relative impacts of RIN and phase noise on the heterodyne receivers. Carrier phase estimation was performed using the QPSK partitioning algorithm in the receiver DSP, as used in above simulations.

The minimum BER versus RIN plots with and without KK linearization are displayed in Fig. 8 (a) and (b) respectively for the case of back-to-back operation at an OSNR of 22 dB. For each point, the minimum BER is obtained at the optimum LOSPR and with the optimum carrier phase estimation block length (which varies with laser linewidth). At negligible RIN levels, i.e. below -170 dBc/Hz, for systems with and without the digital linearization, increased linewidth incurs more phase noise and degrades the performance of the carrier phase estimation algorithm, leading to higher BER. Phase noise dominates the system performance. With the KK receiver, as the RIN increases up to -145 dBc/Hz (Fig. 8 (a)), the BER floor still remains relatively constant at each linewidth level, since the KK scheme allows to use a low LO power, hence reducing RIN-LO beating, as discussed in section IV.A.2. The phase

noise remains the dominant source of penalty. Without digital linearization (Fig.8 (b)), the high LO power required for SSBI mitigation results in high RIN-LO beating interference, and the BER starts to increase even when the RIN is as low as -160 dBc/Hz, and this is the case at all laser linewidths considered. We further plotted the ratio of BER between these two cases with and without applying the KK scheme versus LO RIN at each linewidth value in Fig.8 (c). The reduction in the minimum achievable BER using the KK scheme for SSBI mitigation, and the lower penalty from RIN-LO beating interference can be clearly observed, even in the presence of high laser phase noise.

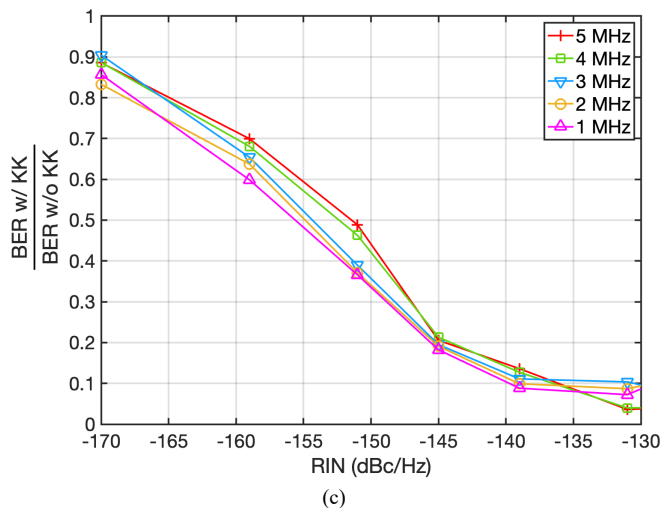
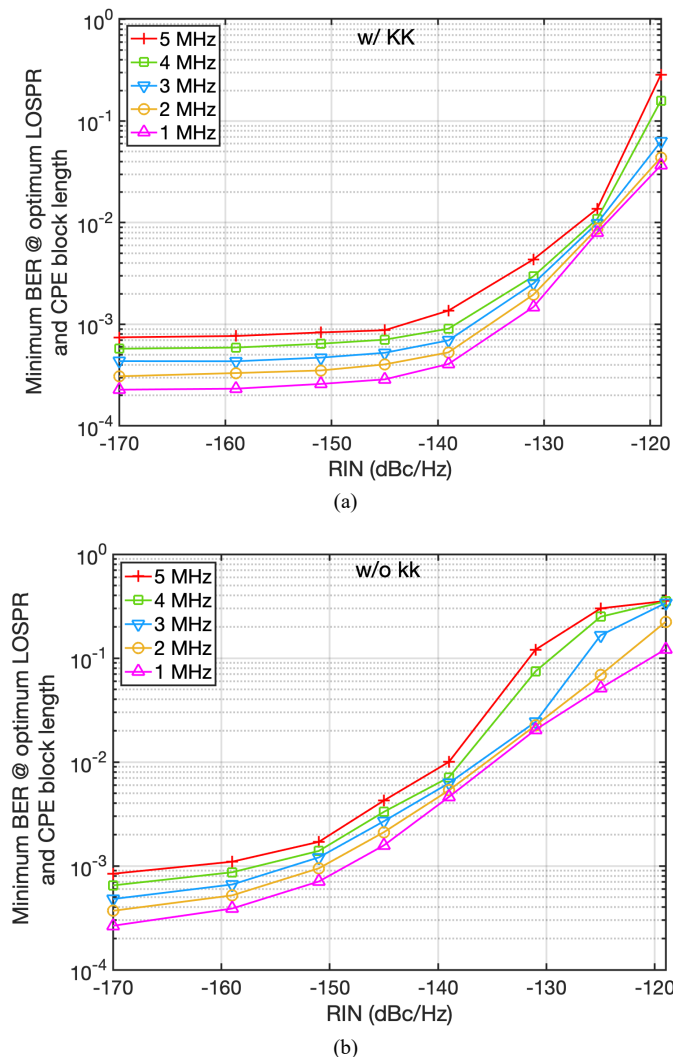


Fig. 8. Minimum BER versus RIN (a) with and (b) without the KK scheme in back-to-back operation at the laser linewidth of 1 to 5 MHz and an OSNR = 22 dB. (c) The ratio of BERs between these two cases (with and without the KK scheme), as a function of RIN for laser linewidths from 1 to 5 MHz.

B. Performance in 80 km transmission system

The system performance in transmission over a link of 80 km of standard single mode fiber (SSMF) was assessed at the same range of RIN levels, laser linewidth (1 MHz) and OSNR (22 dB) as used in the back-to-back simulations described in section IV.A.2. Fiber chromatic dispersion of 17 ps/nm/km was assumed, and receiver-based digital dispersion compensation was applied. The effect of fiber nonlinearity was neglected due to the relatively short distance being considered.

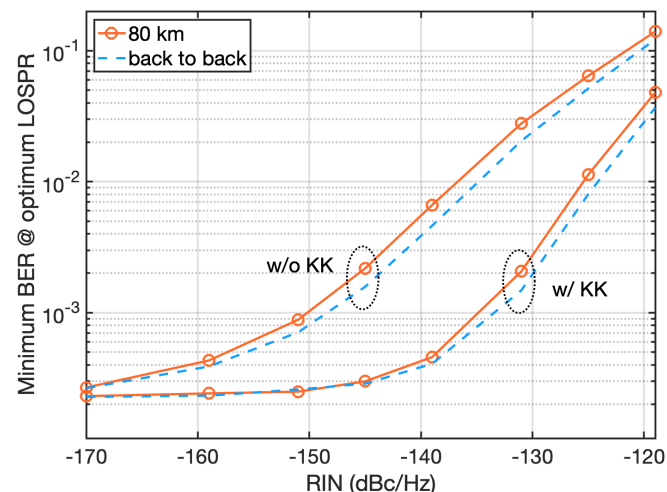


Fig. 9. Minimum BER versus RIN at optimum LOSPRs and OSNR of 22 dB after 80 km transmission.

The BER results versus RIN at optimum LOSPR values at an OSNR of 22 dB, are plotted in Fig. 9 and are compared to the performance in the back-to-back system (from Fig. 7). It can be observed that the system performance is close to that achieved in back-to-back operation, with a slightly higher BER at each RIN level. This is due to the effect known as equalization enhanced phase noise (EPPN). Since the transmitter laser phase noise passes through the dispersive transmission link and the chromatic dispersion compensation module in the receiver DSP, it does not generate additional penalty [29], but for the LO,

which only passes through the chromatic dispersion compensation block, its phase noise may be enhanced by the electronic dispersion compensation [29, 30]. Nevertheless, the impact of the EEPN is observed to be negligible compared to the penalty from the high RIN-LO beating interference, and thus, in transmission over 80 km SSMF, the use of KK linearization still results in a reduction in the minimum BER by over an order-of-magnitude compared to the case of the receiver using high LO power for SSBI suppression.

C. Theoretical model

It is desirable to have an accurate, simple expression to calculate the SNR, and corresponding BER, for the heterodyne single-photodiode-based receiver. For the non-linearized receiver, an SNR equation taking into account only the power of the received electrical signal and the electrical noise powers due to ASE and RIN is found to be inaccurate, due to the nonlinearity of the detection process (i.e., the SSBI is not taken into account in such a simple SNR expression). In the case of the KK receiver, however, the linearization should result in this simple SNR expression being more accurate. In this section, we assess the accuracy of SNR and BER calculations for the KK receiver, considering only the RIN and ASE noise powers.

In this comparison, ideal photodetection was assumed. The phase noise, polarization rotation, differential group delay and corresponding DSP compensation algorithms were switched off.

When the SSBI is fully compensated and the LO power is sufficiently high, the system performance is degraded mainly by the ASE-LO beating interference and the RIN-LO beating interference. Referring to the beating terms defined in (4), the SNR after photodetection can thus be written as:

$$\begin{aligned} SNR &= \frac{P_{signal}}{\sigma_{ASE}^2 + \sigma_{RIN}^2} \\ &= \frac{\langle (2\text{Re}[E_{sig}E_{LO}^*])^2 \rangle}{\langle (2\text{Re}[E_{ASE}E_{LO}^*])^2 \rangle + \langle (2\text{Re}[E_{RIN}E_{LO}^*])^2 \rangle} \end{aligned} \quad (6)$$

where P_{signal} represents the power of the electrical signal, σ_{ASE}^2 and σ_{RIN}^2 are the variances in the electrical signal due to the ASE noise and RIN.

Fig. 10 plots the theoretical SNR obtained using (6), together with the SNR obtained from system simulations, at optimum LOSPRs for different values of RIN and OSNR. It can be observed that the theory and simulation results quite closely match, which indicates that the receiver is operating in a linear manner, with SNR determined primarily by the ASE noise and LO RIN, as assumed in (6). Therefore, in the case of digital linearization with the KK algorithm, (6) can be considered accurate for estimating the received signal SNR with the KK receiver in the presence of the ASE noise and LO relative intensity noise.

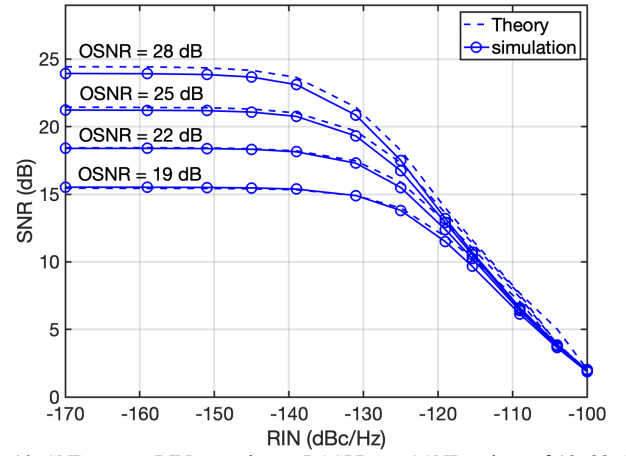


Fig. 10. SNR versus RIN at optimum LOSPRs at OSNR values of 19, 22, 25 and 28 dB.

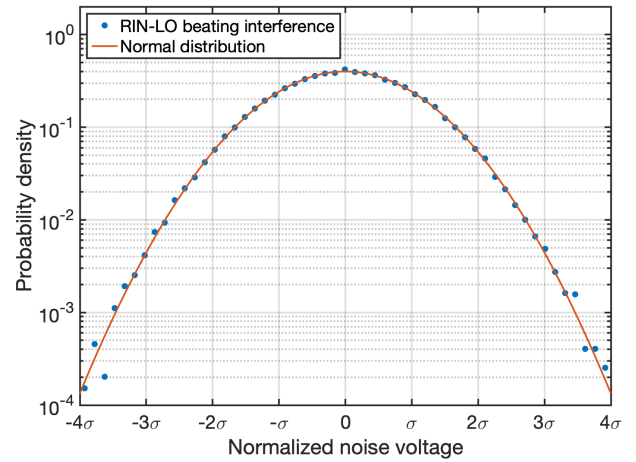


Fig. 11. The probability distribution of RIN-LO beating product.

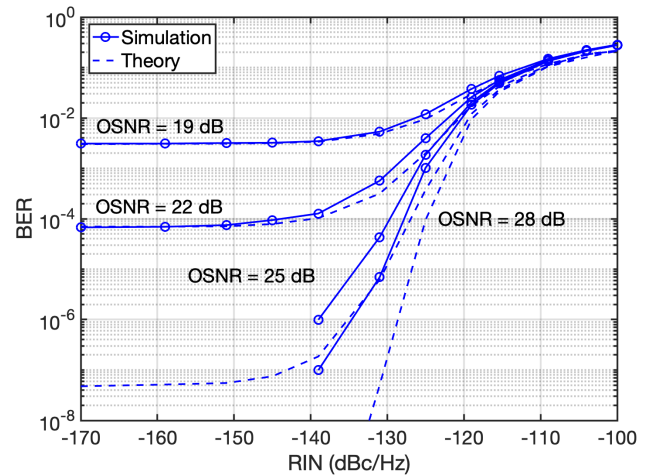


Fig. 12. BER versus RIN at optimum LOSPRs at OSNR values of 19, 22, 25 and 28 dB.

The probability distribution of the RIN-LO beating interference, following the application of the KK algorithm, is shown in Fig. 11, and can be seen to closely follow the normal distribution. Therefore, BER values can be obtained using the complementary error function from the SNRs calculated using (6). The corresponding theoretical BER is plotted in Fig. 12, and

compared with the simulation results. At relatively low OSNRs (i.e., 19 dB and 22 dB), a good agreement between theory and simulations can be observed. However, at high OSNRs of 25 and 28 dB, there are some discrepancies between the simulated BER and the theoretical BER. An explanation for this may be the presence of some residual uncompensated SSBI. Further work is required to investigate this.

D. Discussion

Key conclusions can be drawn from the simulation results described in section A to C, which can be useful in the design and modeling of heterodyne receivers with single-ended photodetectors. Firstly, effective SSBI mitigation is achievable either by using linearization DSP, such as the Kramers-Kronig scheme, or through the use of a high power LO. In the absence of LO RIN, the two techniques achieve similar performance. Secondly, with non-negligible LO RIN, the KK receiver outperforms the receiver without linearization DSP, with an order of magnitude difference in BER being observed between the two at LO RIN levels higher than -140 dBc/Hz, in both back-to-back operation and after transmission over 80 km of standard single mode fiber. Additionally, although low-cost lasers can exhibit high linewidths, the phase noise-induced penalty is smaller than high RIN-LO beating interference in receivers linearized by a high power LO. Therefore, the use of digital linearization (e.g. the KK algorithm) is beneficial in allowing lower amplitude RIN-LO beating products, and consequently, better performance in the case with high RIN, even in the presence of high laser phase noise.

As mentioned in Section II.A, the RIN exhibits a peak near the relaxation oscillation frequency and decays at higher frequencies. It has been suggested to the authors that a guard-band, in the frequency domain, between the LO and the signal could be used, to reduce the penalty from the high spectral power density of the RIN at low frequencies, and also to partially avoid the interference from the RIN-RIN, RIN-LO and signal-signal beating products. To investigate the potential benefits of this approach, we performed further simulations, with a fixed receiver bandwidth and variable symbol rate and FEC overhead. However, it was found that reducing the symbol rate and using a guard band between LO and signal did not achieve a higher net bit rate.

V. CONCLUSION

We investigated the performance of low-complexity heterodyne optical coherent receivers with a single photodiode per polarization, and compared signal-signal beating interference mitigation using two techniques: firstly, using a high power local oscillator and, secondly, employing the Kramers-Kronig digital linearization scheme. A high LO-to-signal power ratio (LOSPR) was found to make the effect of SSBI negligible. In this case, and in the absence of laser relative intensity noise, receivers without digital linearization achieve similar performance to that of KK receivers. In the 28 Gbaud dual polarization 16QAM system considered, at an OSNR of 22 dB, the difference in the required LOSPR for optimum performance was found to be about 20 dB.

An advantage of the low LOSPR of the KK receiver, however, is the reduced impact of LO relative intensity noise.

With local oscillator RIN levels of -140 dBc/Hz and above (typical values for DFB lasers), an order of magnitude lower BER for KK receivers was found to be possible.

This increased tolerance to local oscillator laser RIN achieved using the Kramers-Kronig scheme could be observed even in the presence of the additional penalties arising from high laser phase noise (laser linewidths from 1 to 5 MHz were investigated).

Finally, we showed that, with DSP-based linearization, receiver performance could be accurately predicted using a straightforward SNR calculation, simply taking into account signal, ASE and LO RIN powers, and neglecting the effect of signal-signal beat interference.

REFERENCES

- [1] Cisco, "Cisco Visual Networking Index: Forecast and Methodology 2016-2021," white paper, 2017.
- [2] E. Ip, A. P. T. Lau, D. J. F. Barros, and J. M. Kahn, "Coherent detection in optical fiber systems," *Opt. Express*, vol. 16, no. 2, pp. 753-791, 2008.
- [3] X. Li, Z. Dong, J. Yu, J. Yu, and N. Chi, "Heterodyne coherent detection of WDM PDM-QPSK signals with spectral efficiency of 4b/s/Hz," *Opt. Express*, vol. 21, no. 7, pp. 8808-8814, 2013.
- [4] T. M. Hoang, M. Y. S. Sowailam, M. Morsy-Osman, M. Chagnon, D. Patel, S. Paquet, C. Paquet, I. Woods, O. Liboiron-Ladouceur, and D. Plant, "Transmission of 344 Gb/s 16-QAM Using a Simplified Coherent Receiver Based on Single-Ended Detection," *IEEE Photonics J.*, vol. 8, no. 3, pp. 1-8, 2016.
- [5] R. Elschner, F. Frey, C. Meuer, J. K. Fischer, S. Alreesh, C. Schmidt-Langhorst, L. Molle, T. Tanimura, and C. Schubert, "Experimental demonstration of a format-flexible single-carrier coherent receiver using data-aided digital signal processing," *Opt. Express*, vol. 20, no. 26, pp. 28786-28791, 2012.
- [6] A. Mecozzi, C. Antonelli, and M. Shtaif, "Kramers-Kronig coherent receiver," *Optica*, vol. 3, no. 11, pp. 1220-1227, 2016.
- [7] C. Antonelli, A. Mecozzi, M. Shtaif, X. Chen, S. Chandrasekhar, and P. J. Winzer, "Polarization Multiplexing with the Kramers-Kronig Receiver," *J. Light. Technol.*, vol. 35, no. 24, pp. 5418-5424, 2017.
- [8] A. J. Lowery, L. B. Du, and J. Armstrong, "Performance of optical OFDM in ultralong-haul WDM lightwave systems," *J. Light. Technol.*, vol. 25, no. 1, pp. 131-138, 2007.
- [9] Z. Li, M. S. Erkilinc, K. Shi, E. Sillekens, L. Galdino, B. C. Thomsen, P. Bayvel, and R. I. Killey, "SSBI mitigation and the kramers-kronig scheme in single-sideband direct-detection transmission with receiver-based electronic dispersion compensation," *J. Light. Technol.*, vol. 35, no. 10, pp. 1887-1893, 2017.
- [10] X. Chen, C. Antonelli, S. Chandrasekhar, G. Raybon, J. Sinsky, A. Mecozzi, M. Shtaif, and P. Winzer, "218-Gb/s single-wavelength, single-polarization, single-photodiode transmission over 125-km of standard singlemode fiber using Kramers-Kronig detection," *Opt. Fiber Commun. Conf.*, paper Th5B.6, 2017.

- [11] Z. Li, M. S. Erkılınç, K. Shi, E. Sillekens, L. Galdino, T. Xu, B. C. Thomsen, P. Bayvel, and R. I. Killey, "Spectrally efficient 168 Gb/s/λ WDM 64-QAM single-sideband Nyquist-subcarrier modulation with Kramers-Kronig direct-detection receivers," *J. Light. Technol.*, vol. 36, no. 6, pp. 1340–1346, 2018.
- [12] Y. Zhu, K. Zou, X. Ruan, and F. Zhang, "Single Carrier 400G Transmission With Single-Ended Heterodyne Detection," *IEEE Photonics Technol. Lett.*, vol. 29, no. 21, pp. 1788–1791, 2017.
- [13] S. T. Le, K. Schuh, M. Chagnon, F. Buchali, R. Dischler, V. Aref, H. Buelow, and K. Engenhardt, "8×256Gbps Virtual-Carrier Assisted WDM Direct-Detection Transmission over a Single Span of 200km," *Eur. Conf. Opt. Commun. ECOC*, paper Th.PDP.B.1, 2017.
- [14] S. Fan, Q. Zhuge, M. Y.S. Sowailam, M. Morsy-Osman, T. Hoang, F. Zhang, M. Qiu, Y. Li, J. Wu, and D. Plant, "Twin-SSB Direct Detection Transmission over 80km SSMF Using Kramers-Kronig Receiver," *Eur. Conf. Opt. Commun. ECOC*, paper W.2.D.5, 2017.
- [15] T. Bo and H. Kim, "Kramers-Kronig receiver operable without digital upsampling," *Opt. Express*, vol. 26, no. 11, pp. 13810–13818, 2018.
- [16] X. Chen, C. Antonelli, S. Chandrasekhar, G. Raybon, A. Mecozzi, M. Shtaif, and P. Winzer, "4 × 240 Gb/s Dense WDM and PDM Kramers-Kronig Detection with 125-km SSMF Transmission," *Eur. Conf. Opt. Commun. ECOC*, no. 1, paper W.2.D.4, 2017.
- [17] B. Corcoran, B. Foo, and A. J. Lowery, "Single-photodiode per polarization receiver with signal-signal beat interference suppression through heterodyne detection," *Opt. Express*, vol. 26, no. 3, pp. 3075–3086, 2018.
- [18] M. Seimetz, "High-Order Modulation for Optical Fiber Transmission," Berlin, Germany, Springer, 2009, ch. 2, sec. 2.1.1, pp. 15–17.
- [19] [Online]. Available: <http://nolatech.ru/files/datasheet/DFB-1550-14BF.pdf>, Accessed on: Jan, 31, 2019
- [20] [Online]. Available: <https://media.digikey.com/pdf/Data%20Sheets/Avago%20PDFs/D2547P.pdf>, Accessed on: Jan, 31, 2019
- [21] [Online]. Available: https://www.furukawa.co.jp/fitel/english/active/pdf/signal/ODC-7R001G_FRL15DCWx-A8x-xxxxx-x.pdf, Accessed on: Jan, 31, 2019
- [22] G. P. Agrawal and Niloy K. Dutta, "Semiconductor Lasers," 3rd ed., Norwell, Massachusetts, USA: Kluwer Academic Publishers, 1993, ch. 6, sec. 5, pp. 261–269.
- [23] J. Senior, "Optical Fiber Communications: Principles and Practice," 3rd ed., Harlow, UK, Prentice Hall, 2009, ch. 6, sec. 6.7.4, pp. 356–360
- [24] M. S. Faruk and S. J. Savory, "Digital Signal Processing for Coherent Transceivers Employing Multilevel Formats," *J. Light. Technol.*, vol. 35, no. 5, pp. 1125–1141, 2017.
- [25] B. Zhang, C. Malouin, and T. J. Schmidt, "Design of coherent receiver optical front end for unamplified applications," *Opt. Express*, vol. 20, no. 3, pp. 3225–3234, 2012.
- [26] Z. Li, M. S. Erkılınç, K. Shi, E. Sillekens, L. Galdino, B. C. Thomsen, P. Bayvel, and R. I. Killey, "Joint Optimisation of Resampling Rate and Carrier-to-Signal Power Ratio in Direct-Detection Kramers-Kronig Receivers," *Eur. Conf. Opt. Commun. ECOC*, paper W.2.D.3, 2017.
- [27] [Online]. Available: <http://www.amonics.com/product/44>, Accessed on: Jan, 31, 2019
- [28] [Online]. Available: <https://www.toptica.com/products/wavemeters-laser-diodes/laser-diodes/dfbdbl/>, Accessed on: Jan, 31, 2019
- [29] C. Xie, "Local Oscillator Phase Noise Induced Penalties in Optical Coherent Detection Systems Using Electronic Chromatic Dispersion Compensation," *Opt. Fiber Commun. Conf. Natl. Fiber Opt. Eng. Conf.*, paper OMT4, 2009.
- [30] T. Xu, G. Jacobsen, S. Popov, T. Liu, Y. Zhang, and P. Bayvel, "Analytical estimation in differential optical transmission systems influenced by equalization enhanced phase noise," *Proc. PIERS 2016 Prog. Electromagn. Res. Symp.*, pp. 4844–4848, 2016.